

## Characterisation of a $\text{LaI}_2@(\text{18,3})\text{SWNT}$ encapsulation composite: A 1D $\text{LaI}_2$ crystal fragment, adopting the ‘reduced’ structure of $\text{LaI}_3$

S. Friedrichs,\* J. Sloan,\* R. R. Meyer,\*\* A. I. Kirkland,\*\* J. L. Hutchison,\*\* M. L. H. Green\*

\* Inorganic Chemistry Laboratory, South Parks Road, Oxford, OX1 3QR, United Kingdom

\*\* Department of Materials Science, Parks Road, Oxford, OX1 3PH, United Kingdom

Unprecedented crystal structures are observed when characterising the crystallisation behaviour of materials confined to nanometre-sized cavities, such as the inner cylindrical bore of single-walled carbon nanotubes (SWNT). Encapsulation of lanthanum iodide inside a SWNT revealed a one-dimensional crystal fragment of  $\text{LaI}_2$ , adopting the crystal structure of  $\text{LaI}_3$  with 1/3 of the iodine positions unoccupied. Full characterisation of the encapsulation composite was achieved using an enhanced image restoration technique, which restores the object wave from a focal series of high-resolution transmission electron microscopy (HRTEM) images. The restored object wave provides information about the precise structural data of both filling material and host SWNT, enabling the identification of the SWNT chirality.

Focal series restoration of HRTEM images represents a powerful tool for the complete characterisation of novel nanometre-sized materials. Modification of the image restoration approach, conducted in order to account for rotational movements of the tubular material, enabled the determination of the inclination angle  $\beta$  of the inclusion composite with respect to the image plane, as illustrated in Figure 1 [1]. In this modification, the imaged encapsulation composite is restored in several (here six) individually subregions. Figure 1(a) shows the recombined phase of the encapsulation composite, synthesised by heating SWNTs *in vacuo* in the presence of  $\text{LaI}_3$ , restored from a 20-membered focal series of HRTEM images. Figure 1(b) displays a diagram of the absolute focus values of the individual subregions plotted against their respective centre displacement values along the SWNT axis. A linear fit of the resulting data points (dashed line graph) gave an inclination angle of  $\beta = -17^\circ \pm 10^\circ$ . This inclination angle is consistent with the observation of different projected C-C spacings in each of the SWNT walls, illustrated in the single-pixel line traces in Figure 1(c). Depending on the diameter of the SWNT, its tilt angle  $\beta$  and the observable C-C spacings, the SWNT can be assigned a (18,3) chiral vector, determined by calculation of the cross correlation coefficients (XCFs) between the power spectrum of the imaged tube and the power spectra of a large number of simulated SWNTs under different inclination angles  $\beta$  [2].

The structure and stoichiometry of the encapsulated crystal fragment can be interpreted intuitively, using the restored phase, given in Figure 2(a). Applying a ‘weak-phase object’-approximation, the restored phase shift of each projected column in the imaged object can be regarded proportional to the potential of the inclusion composite, as illustrated in the line traces given in Figure 2. The crystal fragment displays ten well-resolved rows each consisting of three bright dots, running perpendicular to the SWNT axis. The rows are lined up along the tube axis in a staggered arrangement, alternatively shifted towards the left and right tube wall. Diagram 2(1) shows a single-pixel line profile, obtained from a row of the crystal fragment, as indicated by the white line in Figure 2(a).

Computational modelling was applied to find a model corresponding to both the structural motif and the contrast intensities of each column. The final structural model was based on the crystallographic data of bulk  $\text{LaI}_3$  [3], with 1/3 of the iodine atoms omitted to give a crystal fragment with a  $\text{LaI}_2$  stoichiometry, while the remaining atoms maintain their positions in the now ‘reduced’ structure, as indicated in Figure 3(a).

Figure 2(b) displays a simulated phase of the proposed  $\text{LaI}_2@(\text{18,3})\text{SWNT}$  encapsulation composite, illustrating the excellent match of the simulated image regarding both the variation of contrast intensities and projected structural motif for the encapsulated  $\text{LaI}_2$  crystal fragment and the surrounding (18,3) SWNT

References

- [1] S. Friedrichs, J. Sloan, J. L. Hutchison, M. L. H. Green, R. R. Meyer, A. I. Kirkland, *Phys. Rev. B*.64 (2001) 045406.
- [2] R. R. Meyer, S. Friedrichs, A. I. Kirkland, J. Sloan, M. L. H. Green, J. L. Hutchison, *submitted to J. Microsc.*
- [3] W. H. Zachariasen, *Acta Crystallogr.* 1 (1948) 265.
- [4] This research was supported by the EPSRC, the Royal Society, BMBF and Fonds der Chemischen Industry and Hertford College, Oxford.

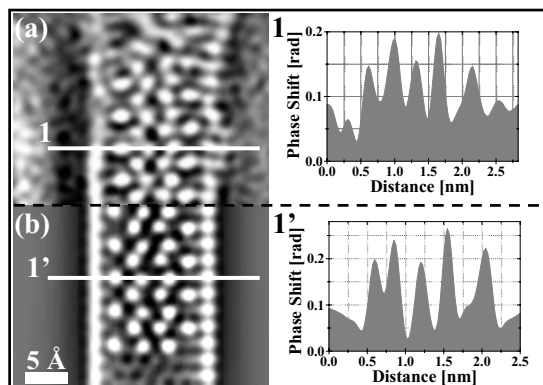


FIG. 2. (a) Selected region of the restored phase, shown in Figure 1(a). (b) Simulated  $\text{LaI}_2@(\text{18,3})\text{SWNT}$  composite. The white lines in Figures (a) and (b) indicate the single-pixel line traces displayed in diagrams (1) and (1') respectively.

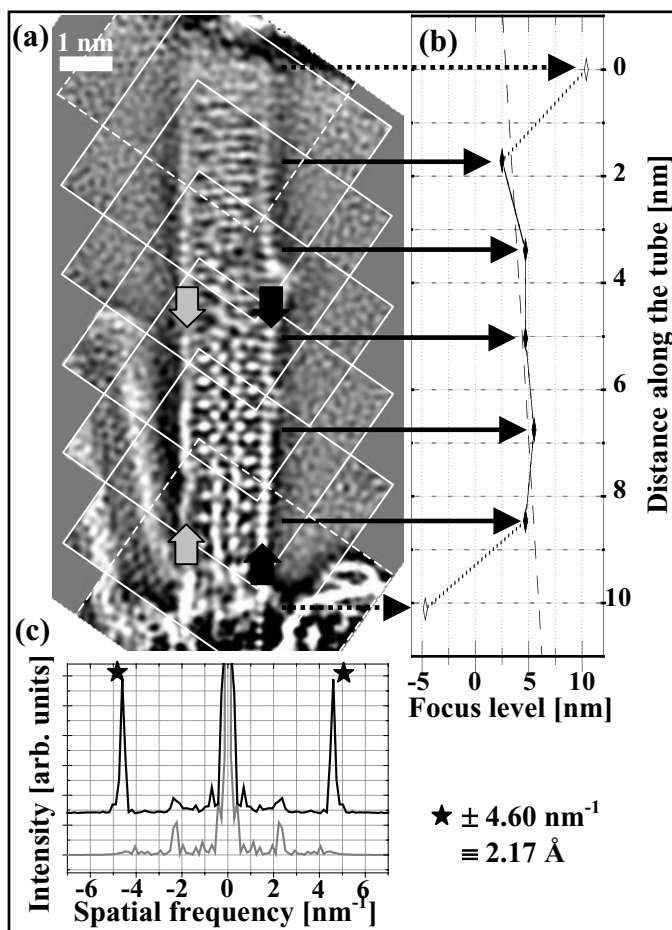


FIG. 1. (a) Restored phase of the imaged encapsulation composite ' $\text{LaI}_2@(\text{18,3})\text{SWNT}$ ', obtained by recombination of six individually restored subregions (white frames). (b) Plot of the defocus value of each subregion versus its centre displacement along the tube axis. (c) Power spectra of line profiles along each of the SWNT walls, indicated by the arrows in Figure 1(a).   
  $\star \pm 4.60 \text{ nm}^{-1} \equiv 2.17 \text{ \AA}$

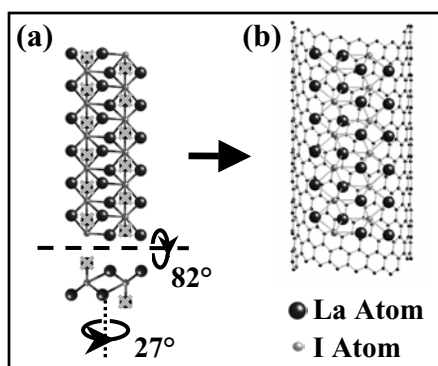


FIG. 3. (a) Modelled fragment of a  $\{100\}$  layer of bulk  $\text{LaI}_3$ ; the iodine atoms missing in the images system are indicated with crosses. (b) Structural model of the proposed  $\text{LaI}_2@(\text{18,3})\text{SWNT}$  (upper SWNT wall omitted for clarity).